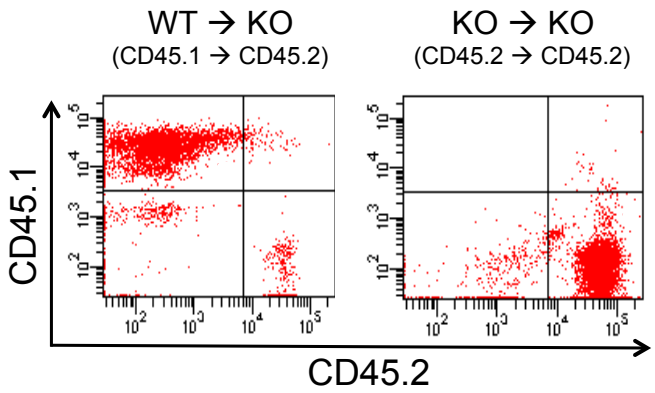

Supplementary Figure 1 | Confirmation of donor cell engraftment in BM chimeric mice. Irradiated uPAR deficient mice (uPAR KO, CD45.2) were received either uPAR WT (B6.SJL, CD45.1) or uPAR KO (CD45.2) BM cells. At 6 weeks after BM transplantation, engraftment of the donor cells was evaluated by flow cytometric analysis of peripheral blood leukocytes stained with fluorescence-conjugated antibodies against CD45.1 (uPAR WT) and CD45.2 (uPAR KO).

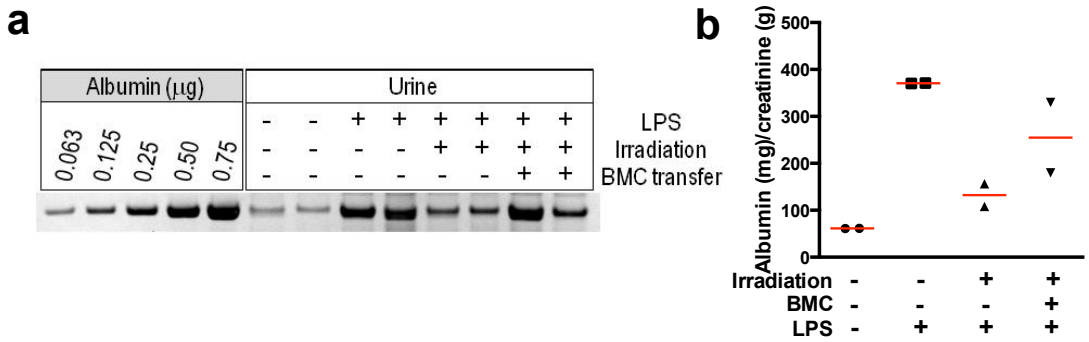

Supplementary Figure 2 | BM cells are responsible for development of proteinuria. (**a**) Urine samples were collected from the mice given i) PBS, ii) LPS, iii) irradiation + LPS, and iv) irradiation + BMC + LPS 24 hours after LPS (or PBS) administration. One microliter of mouse urine resolved on a 10% SDS-PAGE gel. Urinary proteins were stained with Gelcode Blue. Bovine serum albumin (BSA) was used as the standard. (**b**) Bar graph showing albumin/creatinine ratio (ACR) in each group. The intensities of bands shown in (**a**) were measured by densitometric analysis. Albumin levels from urine were calculated using a BSA standard curve (n = 2).

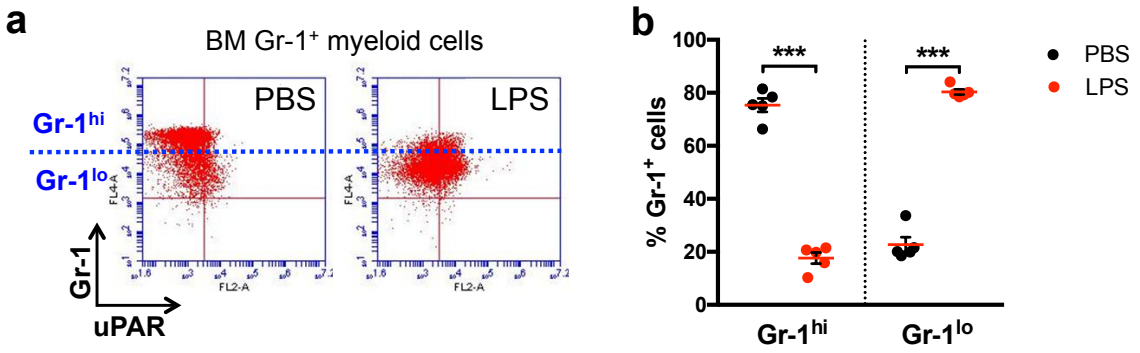

Supplementary Figure 3 | LPS stimulation augmented in the percentage of Gr-1^{lo} cells in BM. BM cells were isolated from PBS- or LPS-treated mice and labeled with fluorescence-conjugated antibodies specific for Gr-1 and uPAR (n = 5 mice per group from two independent experiments). (**a**) Representative dot plots showing uPAR expression and the percentages of Gr-1^{hi} and Gr-1^{lo} cells in the gated Gr-1^{+} BM myeloid cell population. (**b**) The scatter dot plot of the percentages of Gr-1^{hi} and Gr-1^{lo} cells shown in **a**. Data are shown as mean ± SEM; unpaired two-tailed Student's t-test, ***$P < 0.001$.

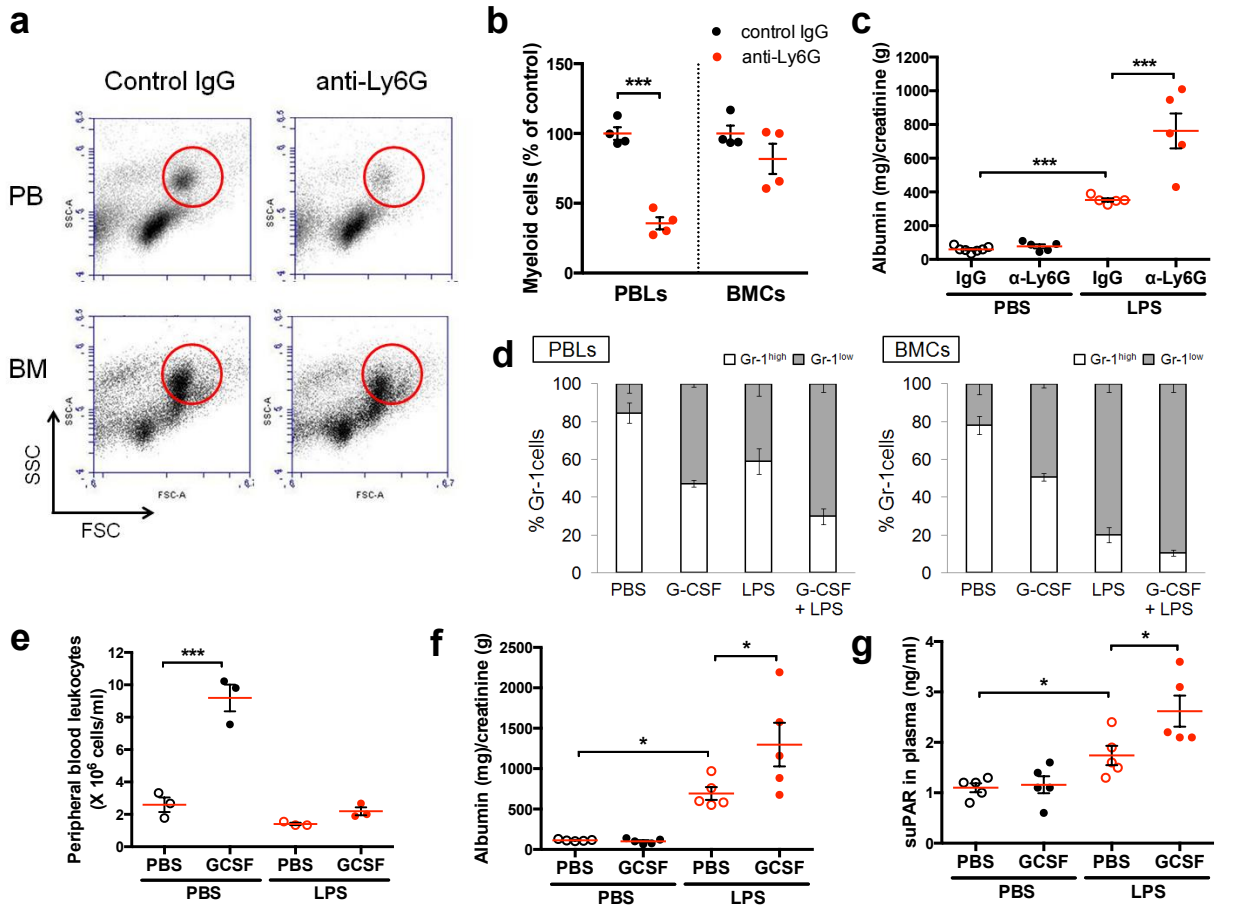

Supplementary Figure 4 | Increased myelopoiesis facilitated LPS-induced proteinuria. (**a-c**) Peripheral blood leukocytes (PBLs) and BM cells were isolated from neutropenic (anti-Ly6G antibody-injected) and control (isotype antibody-injected) BALB/c mice. (**a**) Representative flow cytometry plots of PBLs and BMCs from control IgG or anti-Ly6G antibody injected mice. Myeloid cell populations (red circle) were gated based on their forward scatter (FSC, cell size) and side scatter (SSC, cell granularity) properties (n = 4 per group). (**b**) The scatter dot plot shows quantitative analysis of myeloid cell numbers measured by flow cytometry (n = 4 per group). Data are shown as mean ± SEM; unpaired two-tailed Student's t-test, ***$P < 0.001$. (**c**) ACR levels. The results are from two independent experiments (n = 7 for IgG+PBS, n = 5 for α-Ly6G+PBS, IgG+LPS, and α-Ly6G+LPS). Data are shown as mean ± SEM. One-way ANOVA, Tukey's multiple comparison test, ***$P < 0.001$. (**d-g**) BALB/c mice were treated with G-CSF (or PBS) for two consecutive days prior to LPS (or PBS) stimulation. Blood and bones (femurs and tibias) were collected 24 hours after LPS administration. (**d**) PBLs and BMCs were isolated and labeled with fluorescence-conjugated antibodies specific for Gr-1. The bar graphs show percentages of Gr-1^{high} and Gr-1^{low} cells in the total Gr-1^{+} cells. (**e**) The scatter dot plot shows quantitative analysis of white blood cell (WBC) counts determined using a Hemavet (n = 3 per group). Data are shown as mean ± SEM. One-way ANOVA, Tukey's multiple comparison test, ***$P < 0.001$. (**f**) Proteinuria. (**g**) Plasma suPAR levels. In **f**, **g** n = 5 per group. Data are shown as mean ± SEM. One-way ANOVA, Tukey's multiple comparison test, *$P < 0.05$.

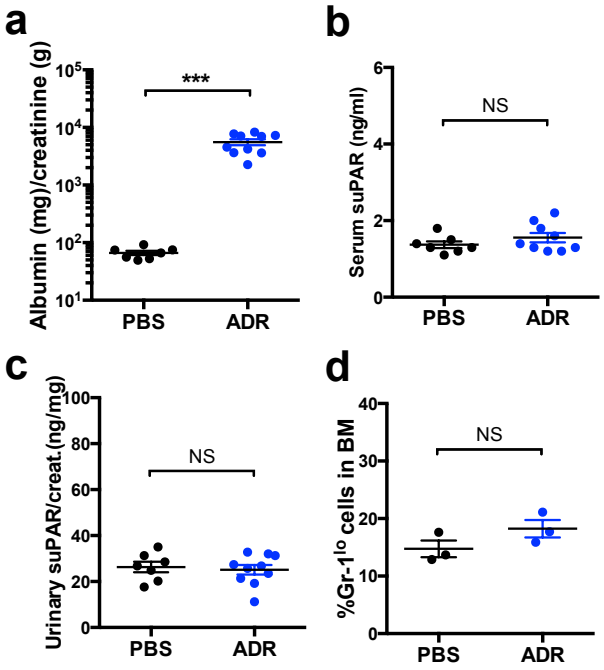

Supplementary Figure 5 | Proteinuria in Adriamycin (ADR) model did not correlate neither with suPAR levels nor Gr-1^{lo} BM cells. Male BALB/c mice were injected with ADR via the tail vein at a dose of 11 mg per kg body weight. Six days after ADR injection, urine and blood samples were collected and femurs, and tibias were harvested from the sacrificed mice. (**a**) Proteinuria. (**b**) Plasma suPAR levels. (**c**) Urinary suPAR levels. (**d**) Percentage of Gr-1^{lo} BM myeloid cells. In **a** $n = 7$ for PBS, $n = 10$ for ADR; in **b** $n = 7$ for PBS, $n = 9$ for ADR; in **c** $n = 7$ for PBS, $n = 10$ for ADR, in **d** $n = 3$ per group. Data are shown as mean ± SEM; unpaired two-tailed Student t-test, ***$P < 0.001$, NS, not significant.

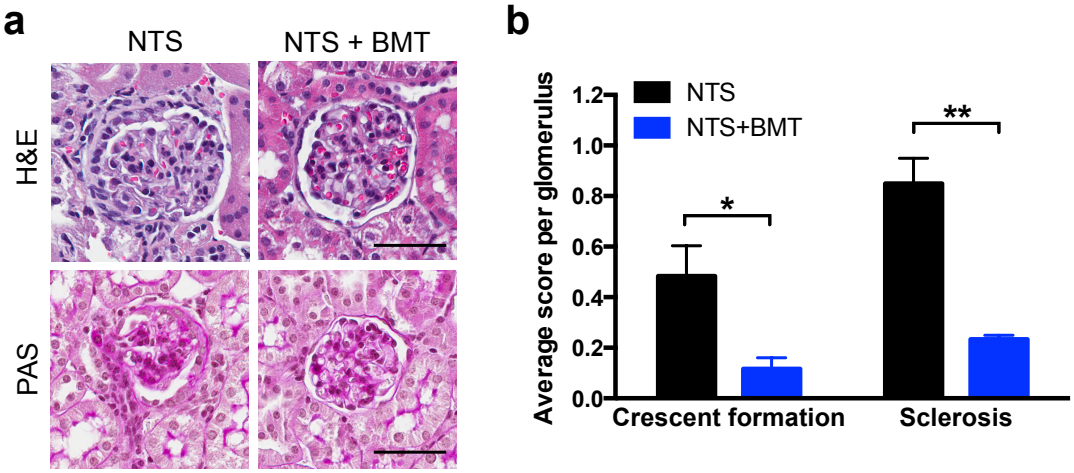

Supplementary Figure 6 | BMT ameliorated NTS-induced renal damage. (**a**) Sections of formalin-fixed kidney glomeruli from the NTS-injected mice receiving PBS (NTS + vehicle) or BMT (NTS + BMT) were stained with H&E and with PAS. Scale bars, 50 μm. (**b**) Glomerular crescent formation and sclerosis were evaluated in a blinded fashion on PAS-stained paraffin sections and scored using a semiquantitative scale (0-3), in which 0 represented no abnormalities, and 1, 2, and 3 represented mild, moderate, and severe abnormalities, respectively. Ten glomeruli were assessed for each animal (n = 3 per group). Data are shown as mean ± SEM; unpaired two-tailed Student t-test, *$P < 0.05$, **$P < 0.01$.

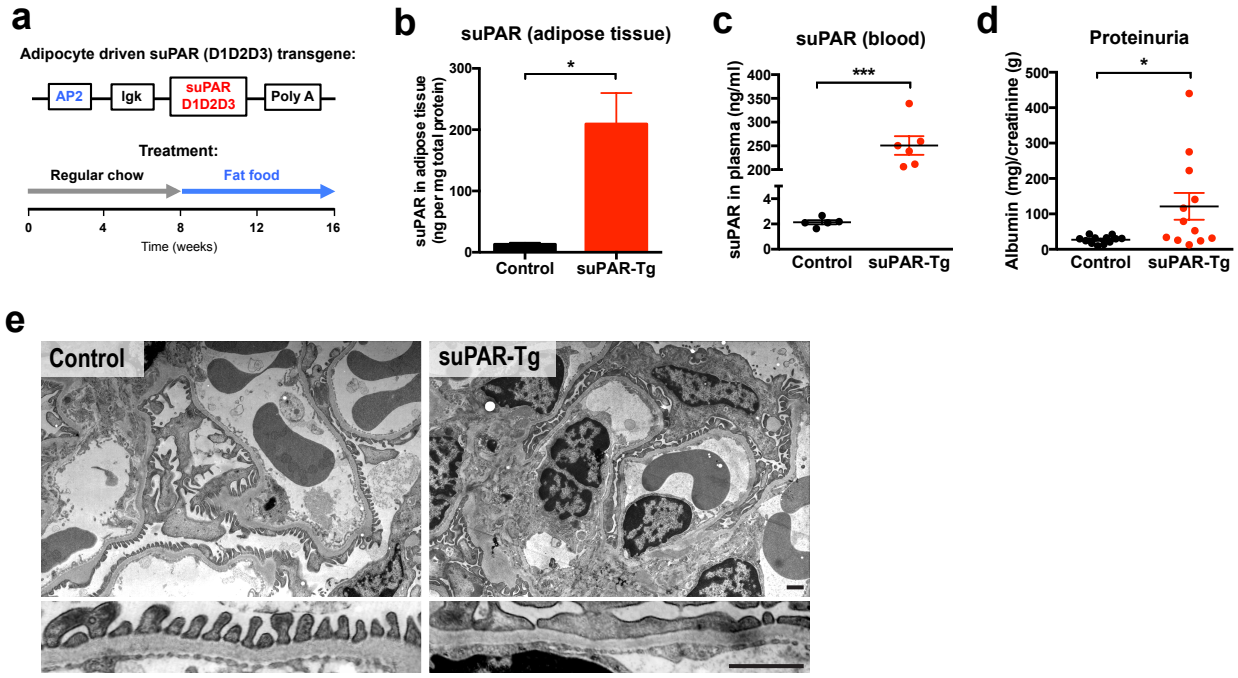

Supplementary Figure 7 | Long-term exposure of suPAR resulted in podocyte injury and proteinuria in suPAR transgenic mice. (**a**) Generation of a novel suPAR transgenic mouse (suPAR-Tg) model overexpressing the soluble form of mouse full-length suPAR (corresponding to NP_035243, DIDIIDIII without GPI anchor) in adipose tissue using the aP2 promoter. The suPAR transgene is secreted into the circulation owing to the absence of GPI anchor. To enhance suPAR production, regular rodent diet was replaced by high fat food when the suPAR-Tg (n = 12) and non-Tg littermate controls (n = 12) were at least 2 months old and the animals were kept on the high fat diet for 8 weeks. After 8 weeks of high fat diet feeding, urine and blood samples were collected and kidney and visceral fat tissues were harvested from the sacrificed mice. (**b**) Adipose tissue-specific expression of the suPAR transgene was confirmed by performing ELISA using lysates of visceral fat tissues (n = 3 per group). Data are shown as mean ± SEM; unpaired two-tailed Student t-test, $*P < 0.05$. (**c**) Plasma level of suPAR. (**d**) Proteinuria development. In **c** n = 5 for control, n = 6 for suPAR-Tg; in **d** n = 12 per group. Data are shown as mean ± SEM; unpaired two-tailed Student t-test, $*P < 0.05$, $***P < 0.001$. (**e**) TEM images (10,000X) displaying podocyte foot processes were enlarged and highlighted. Scale bars, 1 μm.

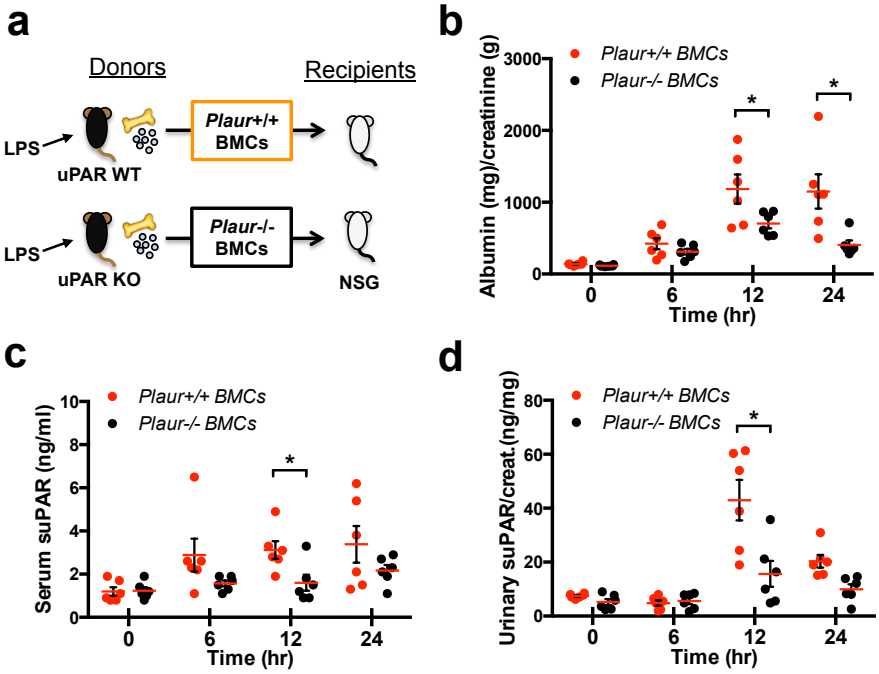

Supplementary Figure 8 | uPAR deficient BM cells had a limited disease-transfer ability. WT and *Plaur*$^{-/-}$ (KO) mice were challenged with LPS for 24 hours, and then BM cells were isolated from those mice and transferred into NSG mice. ACR and suPAR levels were monitored in a time course (n=6 per group from two independent experiments). (**a**) Schematic experimental design. (**b**) Proteinuria. (**c**) Serum suPAR levels. (**d**) Urinary suPAR levels. Data are shown as mean ± SEM (**b**-**d**); unpaired two-tailed Student t-test, *$P < 0.05$.

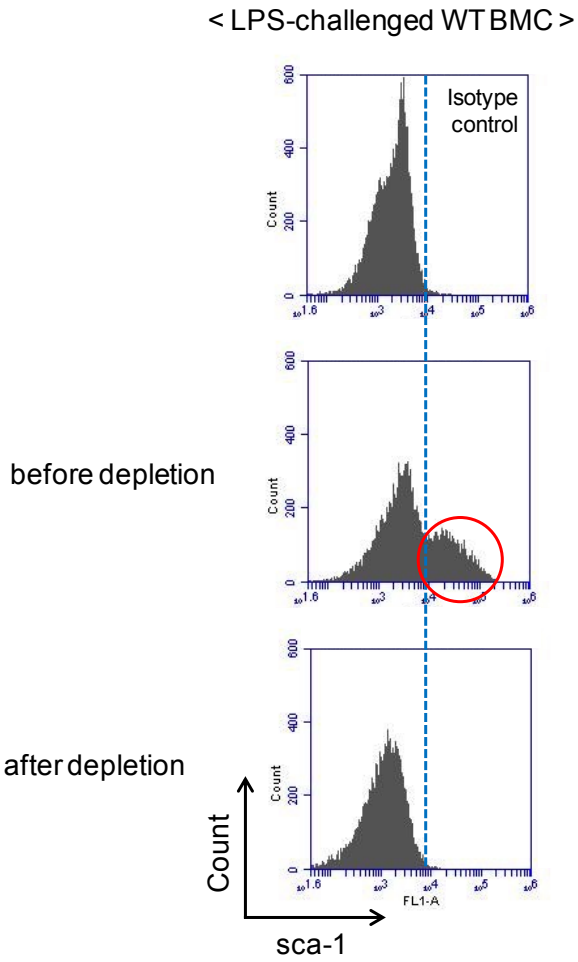

Supplementary Figure 9 | Confirmation of Sca-1$^+$ cell depletion. BM cells were isolated from WT mice treated with LPS. Sca-1$^+$ cells were removed from whole BMCs by magnetic separation. Cells were stained with FITC conjugated anti-Sca-1 or isotype control antibodies. Representative histograms display the expression profiles of Sca-1 (n = 2). Blue dashed line indicates the cutoff for a positive Sca-1 signal. Sca-1-positive cells are encircled in red.

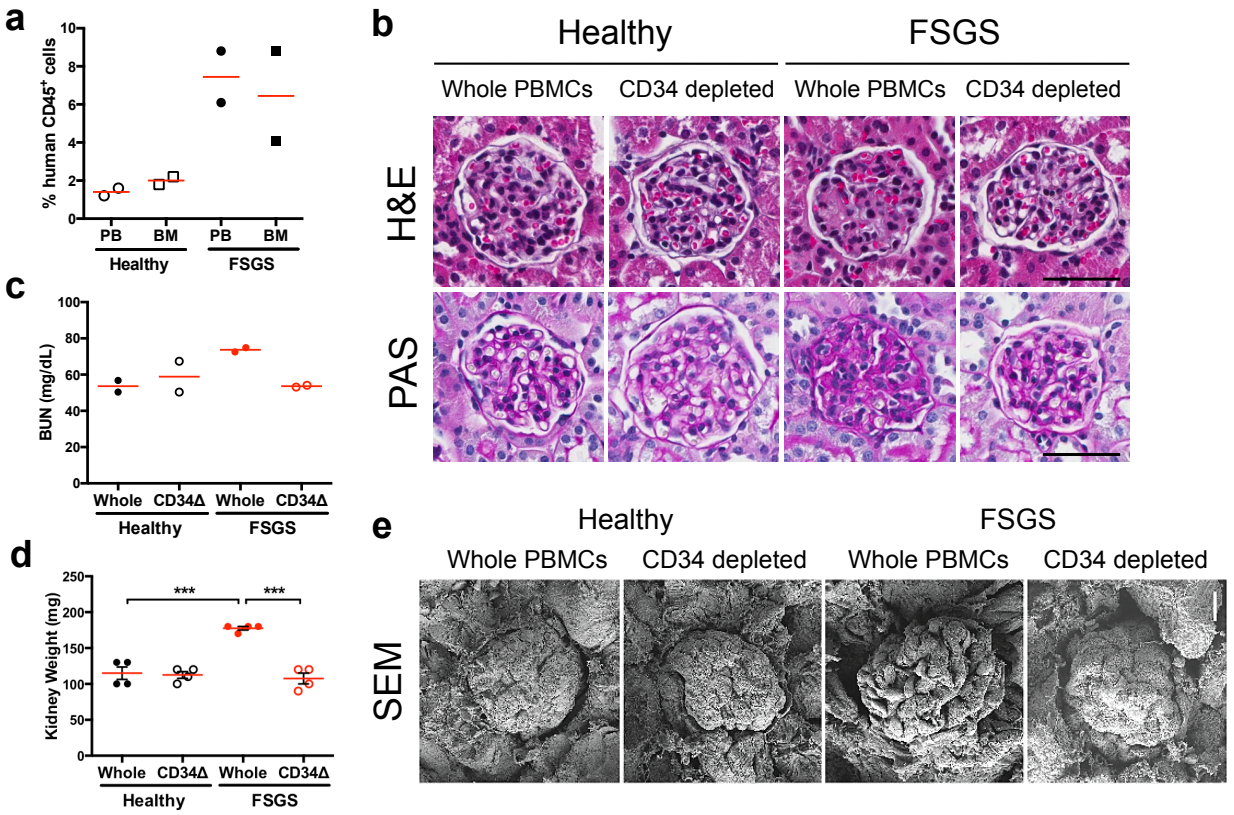

Supplementary Figure 10 | Kidney functions in the xenograft mice. (**a**) Engraftment rates of human cells were determined by the percentage of human $CD45^+$ cells in peripheral blood (PB) and BM of the xenograft mice at 12 weeks post engraftment. $n = 2$ per group. (**b**) Sections of formalin-fixed kidney glomeruli from the xenograft mice were stained with H&E and with PAS. Scale bars, 50 μm. (**c**) Blood urea nitrogen (BUN), as a marker for kidney function, was measured in serum samples from the humanized mice using a colorimetric-based assay kit (BioAssay Systems). $n = 2$ per group. (**d**) Kidney weight. $n = 4$ per group. Data are shown as mean ± SEM. One-way ANOVA, Tukey's multiple comparison test, $^{***}P < 0.001$. (**e**) Representative SEM images of whole glomeruli of the xenograft mice. Scale bar, 10 μm.

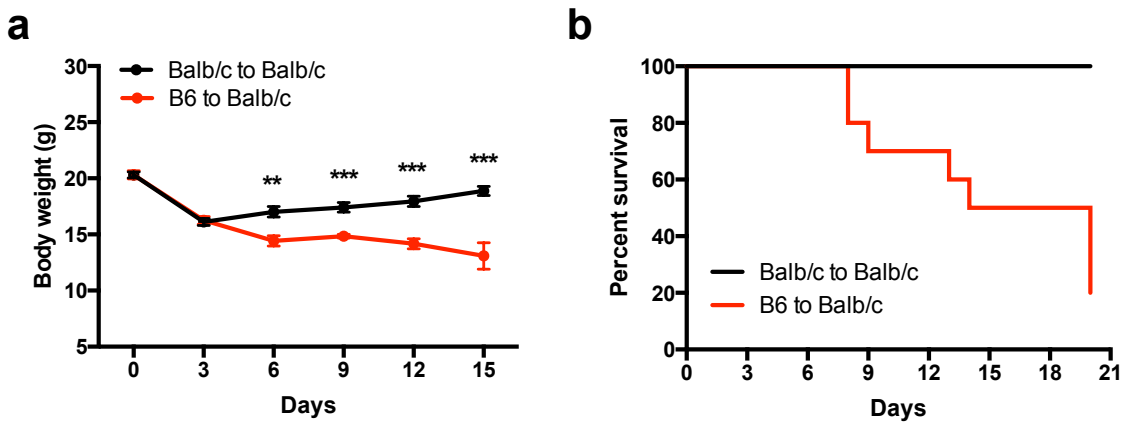

Supplementary Figure 11 | Body weight and mortality in a mouse model of GVHD. BALB/c recipients were lethally irradiated (9.5 Gy) and received 10^7 BM cells and 5 X 10^6 spleen cells from C57BL/6 donors (MHC mismatched allogeneic transplant; B6 to BALB/c, n = 10) via retro-orbital injection. As a control (syngeneic transplant; BALB/c to BALB/c, n = 7), irradiated BALB/c recipients received BM cells and spleen cells from BALB/c donors. Mice were monitored for body weight (**a**) and mortality (**b**). Data are shown as mean ± SEM; unpaired two-tailed Student t-test, $^{**}P < 0.01$, $^{***}P < 0.001$.

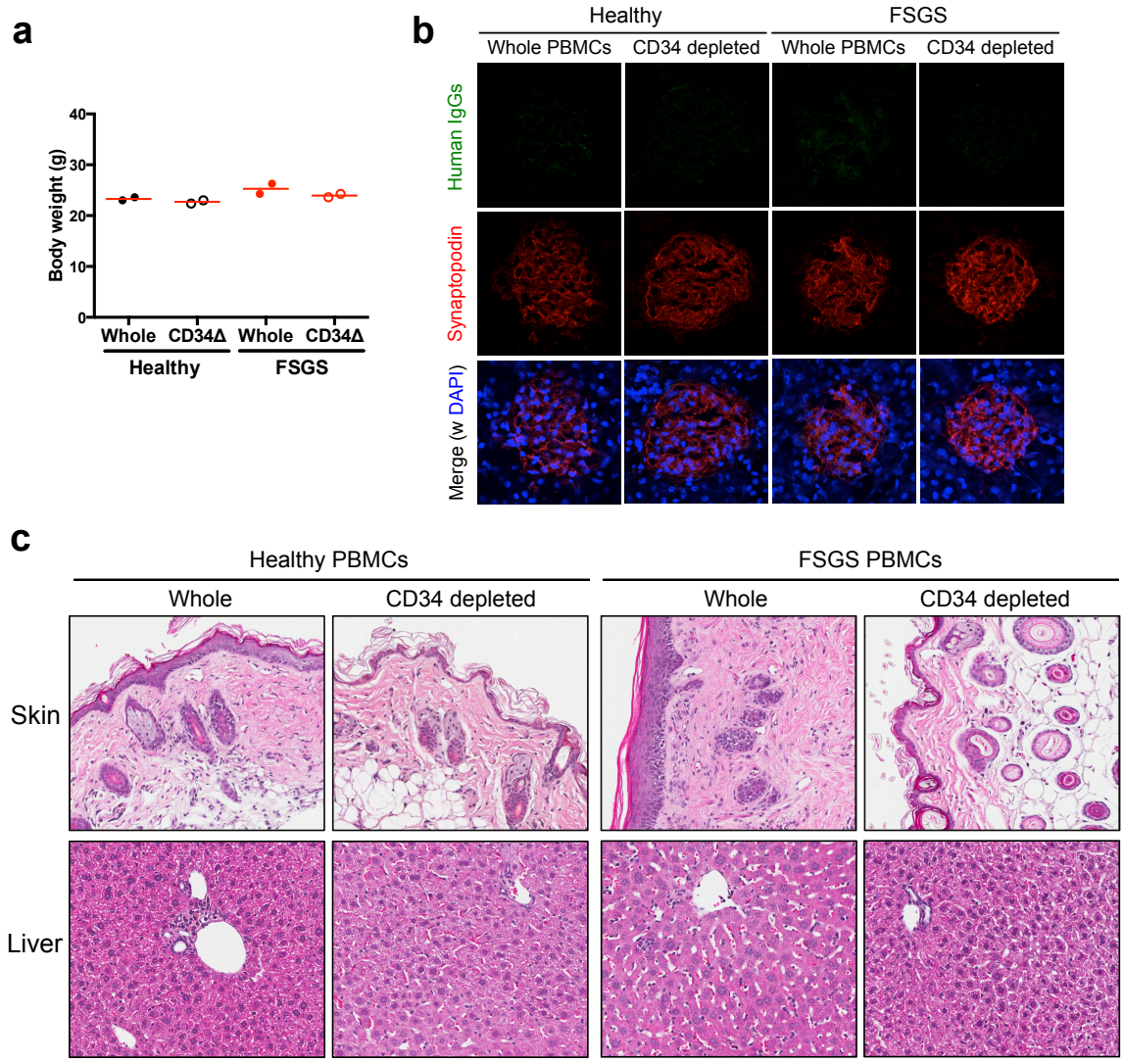

Supplementary Figure 12 | GVHD was not a major cause of renal dysfunction observed in the xenograft mice. (**a**) Body weights (g) of the xenograft mice. n = 2 per group. (**b**) Representative immunofluorescent images of glomeruli stained with human IgG (green), synaptopodin (glomerular marker, red), and DAPI (blue). (**c**) Representative images of H&E-stained skin and liver sections from the xenograft mice.